Impact of climate change on hydrologic components using CORDEX Africa climate model in Gilgel Gibe 1 watershed Ethiopia

Tamene Adugna Demissie

Faculty of Civil and Environmental Engineering, Jimma University, Jimma, 378, Ethiopia

ARTICLE INFO

ABSTRACT

This study aimed to assess the impact of climate change on the hydrological components of Gilgel Gibe-1 using the ensemble of Coordinated Regional Climate Downscaling Experiments (CORDEX) Africa Domain namely REMO2009, HIRAM5, CCLM4-8 and RCA4 Regional Climate Models (RCMs) simulations. The performance of these RCM models was evaluated using the observed data from 1985 to 2005 and the ensemble was shown to simulate rainfall and air temperature better than individual RCMs. Then the RCMs ensemble data for historical and future projections from 2026 to 2055 years under RCP4.5 and RCP8.5 were corrected for bias and used to evaluate the impact of climate change. A non-linear bias correction and the monthly mean biases corrections method is used to adjust precipitation and temperature respectively. The future projection shows that; rainfall is expected to increase from August to December with maximum values of 1.97–235.23% under RCP4.5. The maximum temperature is expected to increase with maximum value of 1.62 °C under RCP8.5 in the study area. The calibrated and validated Soil and Water Assessment Tool (SWAT) model was used to investigate the impact of climate change on hydrologic components such as surface runoff, lateral flow, water yield, evapotranspiration and sediment yield. The SWAT model was calibrated and validated using monthly stream flow with the statistical performance of R^2 value of 0.82 and NSE value of 0.72 for calibration and R^2 of 0.79 and NSE of 0.67 for validation. Surface runoff and sediment yield are expected to increase from August to December under RCP4.5 and from August to February under RCP8.5. Overall both surface runoff and sediment yield are expected to increase in the future.

1. Introduction

Climate change has become as one of the most pressing issues of the twenty-first century. One of the most significant natural cycles, the hydrological cycle, is strongly influenced by climate change, which has led to much research into those consequences [1,2]. The changes in the hydrological conditions resulted in a variety of consequences on water resource systems around the world [3,4]. Anthropogenic greenhouse gas emissions, which ultimately lead to an increase in the earth's surface temperature, are the causes of climate change [5].

The IPCC 2021 report indicated that the global surface temperature has increased faster since 1970 than in any other 50-year period over at least the last 2000 years (high confidence). Temperatures during the most recent last decade (2011–2020) surpassed those of the most recent multi-century warm period, around 6500 years ago (0.2 °C–1 °C relative to 1850–19000) (medium confidence). Heavy precipitation events have increased in frequency and intensity since the 1950s over most land areas for which observational data are
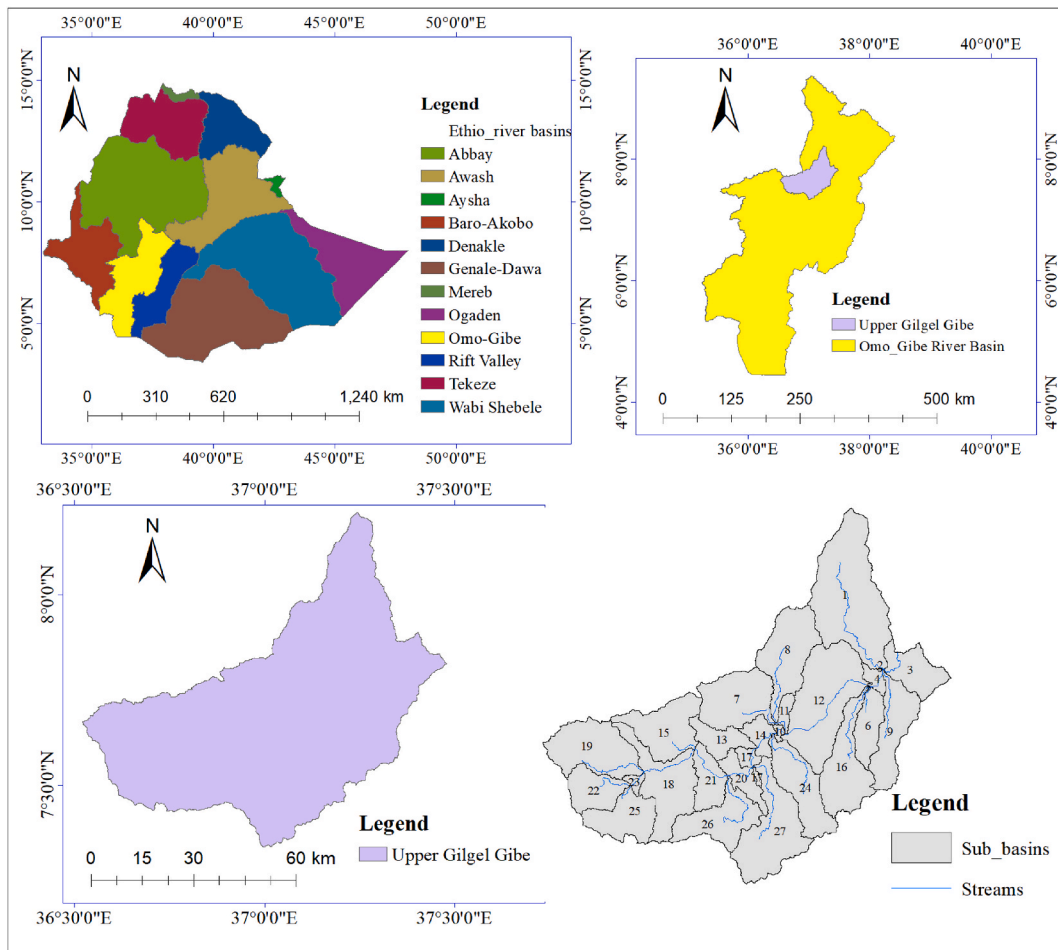
Fig. 1. Map of the study area.

sufficient for trend analysis (high confidence), and human-induced climate change is likely the dominant cause, and contributing to the increase in agricultural and ecological droughts in some regions due to increased land evapotranspiration (medium confidence) [6].

Developing countries face several water resource management challenges due to climate change [7,8]. Poverty and inadequate adaptive capacity make developing countries, such as those in Sub-Saharan Africa, particularly vulnerable [9].

In the Gilgel Gibe −1 watershed, the problems such as deforestation and land degradation due to poor land management techniques, combined with changes in hydro-climatic variables, pose a significant threat to the lifespan of the reservoir [10]. The Gilgel Gibe-1 watershed is one of the sub-basins of the upper Omo-Gibe catchment that is prone to soil erosion. The dam for the Gilgel Gibe-1 hydroelectric power was built in this watershed. Sediment-laden streamflow reveals the extent of land degradation in the upstream watershed and the siltation problem at the downstream Gilgel Gibe-1 hydropower reservoir [11]. Therefore, an assessment of the impact of climate change on hydrological components such as surface runoff and sediment yield is required to address issues related to the Gilgel Gibe-1 hydropower reservoir water management.

Several studies on the impact of climate change using climate models have been conducted worldwide [12]. Results from Global Circulation Models (GCM) and downscaling techniques for bias correction are used to investigate the impact of climate change. However, several studies used RCMs for climate impact studies [13–15] due to RCM improved model simulation for regional investigations when compared to GCM [16,17]. Due to its higher resolution than GCM (approx. 25–50 km), RCM is better suited for areas with complex physiographical features [18]. This study also used RCMs to assess the effects of climate change.

The IPCC issued the RCP i.e. 2.6, 4.5, 6.0, and 8.5 scenarios for projected greenhouse gas emissions, which have been employed in hydrological studies [19]. RCP4.5 is an intermediate scenario, with emissions peaking at about 2040 and subsequently declining. RCP8.5 refers to the carbon concentration that causes global warming of 8.5 W per square meter on average [5]. The studies in Africa mainly used CORDEX RCM under RCP4.5 and RCP8.5 to study the effects of climate on hydrology [7,20,21].

In Ethiopia, some studies have used the CORDEX RCM model to assess the influence of climate change on watershed sediment output and other hydrological components. For instance, Refs. [22–24], used the CORDEX RCM model. In addition, [25] used CORDEX Africa RCM under RCP4.5 and RCP 8.5 to study the hydrological response of the watershed to combined land use/land cover and
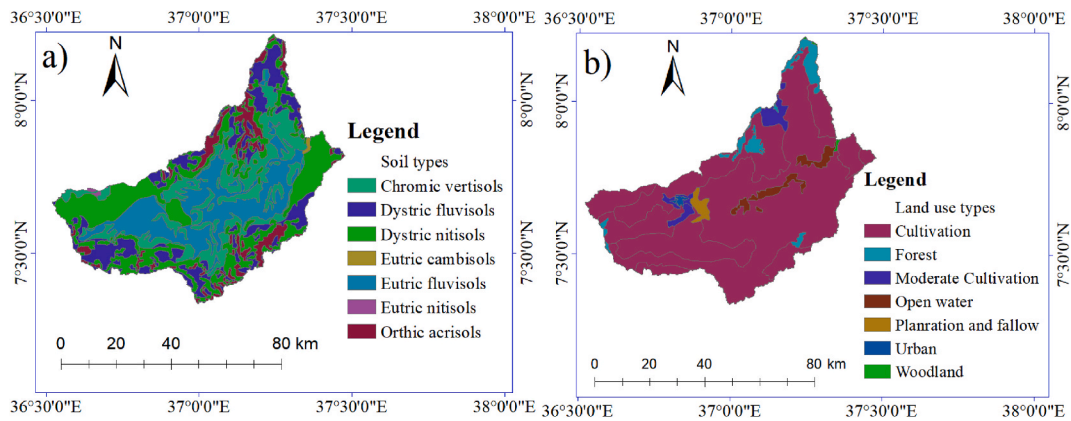
Fig. 2. (a) Soil map and (b) Land use Land Cover of Gilgel Gibe-1 Watershed.

climate change. All of the above researches were carried out in the Awash, Upper Blue Nile, and Central Rift valley basins. No climate change impact studies on hydrological processes using CORDEX Africa RCM in the Gilgel Gibe-1 watershed have been conducted.

The selection of climate models depends on their ability to simulate both historical simulations and future projections [26]. This study is based on [15]. Ref. [15] evaluated the performance of four RCMs models such as REgional MOdel (REMO2009), High-Resolution Hamburg Climate Model 5 (HIRAM5), Climate Limited-Area Modeling Community (CCLM4-8) and Rossby Center Regional Atmospheric Model (RCA4) simulations from the CORDEX Africa program in terms of their ability to reproduce past rainfall and air temperatures, showing that the ensemble of the RCMs models performed well over southwest Ethiopia, particularly in the Gilgel Gibe-1 watershed. These models have also been evaluated in several studies across Africa [27–29] and showed good results in simulating rainfall and air temperature. Hence, in this study, to examine the influence of climate change on the hydrological components, a bias-adjusted ensemble of these models was utilized as an input to the SWAT hydrological model. The Soil Water Assessment Tool (SWAT) model is one of several hydrological models developed to predict hydrological components. It has shown its robustness in predicting sediment yield in different catchment areas under different basin characteristics and can be reliable in estimating and predicting hydrological components [22].

Assessing the impacts of climate change on hydrological components at the watershed and sub-basin level will assist governmental and non-governmental organizations involved in watershed planning and management.

2. Materials and methods

2.1. Description of the study area

The Gilgel Gibe River is one of the major tributaries of the Great Gibe River, and it originates in the mountainous areas of Seka woreda of the Jimma zone. Before joining the Gilgel Gibe-1 reservoir, it collects discharges from Seka, Jimma, Serbo, and Asendabo towns. The Gilgel Gibe-1 watershed is located between 6.16° to 8.31° N latitude and 36.69° to 37.62° E longitudes. It has a total catchments area of 4220 km². Fig. 1 indicated the map of the study area.

2.2. Data collection and analysis

In order to analyze and provide an output, the SWAT hydrological model requires both spatial and daily weather data as inputs. The Digital Elevation Model (DEM), the soil map and the land use/land cover map are the required spatial data. Rainfall, maximum and minimum temperature, solar radiation, relative humidity and wind speed are required as input data. One of the data needed to calibrate and validate the SWAT model is stream flow. Recorded stream flow is also required to calibrate and validate the SWAT model.

2.2.1. Digital elevation model (DEM)

For this study, the DEM with a grid resolution of 12.5 m by 12.5 m is downloaded from the website: https://vertex.daac.asf.alaska.edu/and used to generate the topography of the basin. The watershed's topography denotes the arrangement of natural and man-made characteristics. From upstream to downstream, the geography of the Gilgel Gibe-1 watershed region declines in elevation. The lowest elevation is 1642 m near the watershed's outlet, while the highest elevation is 3345 m in the mountainous area along with the river's sources.

2.2.2. Soil types and land use land cover of Gilgel Gibe-1 watershed

The Ministry of Water Resources, Irrigation, and Electricity (MoWIE) provided the soil and Land use/Land cover data which are highly relevant for the SWAT model. The Gilgel Gibe-1 watershed has seven different soil types (Fig. 2a). Chromic vertisols, Dystric fluvisols, Dystric nitisols, Eutric cambisol, Eutric fluvisols, Eutric nitisols and orthic acrisols. Eutric Nitosols (Ne) dominate among the

soil types available in the watershed. Eutric Nitosols are Nitosols with a base saturation of 50% or more. They are found on almost flat to sloping terrain in the highlands of Ethiopia (http://ethiopiamountain.com).

Land use/Land cover is one of the most important factors affecting runoff, evapotranspiration, and surface erosion in a watershed. The major land use/land cover in the Gilgel Gibe-1 watershed are: Highly Cultivated, moderately cultivated, forest, Urban, open water, woodland, plantation, and fallow as shown in Fig. 2b.

2.2.3. Climate data

The meteorological stations utilized in this study were chosen based on data availability and overall study area representativeness. Jimma (located at $7^0 40'12''$ N latitude and $36°49'12''$ E longitude), Assendabo (located at $7°45'0''$ N latitude and $37°13'12''$ E longitude), and Sekoru (located at $7°55'12''$ N latitude and $37°25'12''$ E longitude) were the meteorological stations chosen. Long-term observations are critical for understanding local and regional climate and climate change, as well as hydrological planning and decision-making [30].

In this study, weather data which spanned 30 years from 1988 to 2017 obtained from the Ethiopian National Meteorological Service Agency (ENMA) were used to set up the SWAT model. Streamflow data recorded for 15 years (1990–2004) at a gauging station near Asendabo (near the outlet of Gilgel Gibe1 reservoir) was collected from the Ethiopian Ministry of Water Resources, Irrigation, and Electricity and used to calibrate and validate the SWAT hydrological model.

Daily precipitation and temperature RCMs (CORDEX) Africa domains such as CCLM4-8, HIRHAM5, REMO2009 and RCA4 provided by data of the two illustrative concentration pathways (RCP) mid-range mitigation emission (RCP4.5) scenarios and high emission scenario (RCP8.5) were selected for their good performance in Ethiopia and East Africa. The RCMs have a spatial resolution of $0.44° * 0.44°$ and extracted using the latitude and longitudes of the selected stations, checked for performance, bias corrected and used for climate change impact on hydrological components.

The performance of CORDEX RCMs these models: HIRHAMS5, REMO2009, RCA4, and CCLM4-8 in simulating rainfall and air temperature across southwest Ethiopia, specifically in the Gilgel Gibe-1 watershed, were evaluated using observed weather data from 1985 to 2005. The results of the performance evaluation of these models demonstrated that the ensemble of all models outperformed the individuals [15]. Consequently, in this study, the bias-corrected historical simulated daily rainfall and air temperature ensemble data from these RCMs were used as input to simulate baseline hydrological parameters, and similarly the ensemble of bias-corrected projected air temperature and rainfall of these RCMs under RCP4.5 and RCP8.5 for a future period of (2026–2055) were used to simulate future hydrological parameters.

The Percentage mean of Bias (PBIAS), Pearson's Correlation Coefficient (r), and Root Mean Square Error (RMSE) were used to assess the effectiveness e of different RCMs in simulating precipitation and temperature [15,31]. The ensemble data from these models were bias-corrected in this work to reduce the input error.

Bias correction for climate data has been frequently used [32]. A non-linear bias correction method is most commonly used to adjust the simulated precipitation data from RCM. It is of the form of $P^{**} = aP^b$. In which: P^{**} is the bias-corrected daily rainfall; P is the biased daily rainfall and a and b are the transformation coefficients [33]. For the temperature bias correction, the monthly mean biases corrections are calculated according to equation of [24,34].

$$T^{xx} = \overline{Ti}^{obs} + \frac{s(Ti^{obs})}{s(Ti^{mod})}(\overline{Ti}^{mod})$$

where T is the modeled day-temperature, T^{xx} is the corrected temperature, Ti^{obs} and $\overline{Ti}^{mod}$ is the mean temperature in a month i and $s(Ti^{obs})$ and $s(Ti^{mod})$ is the standard deviation of the daily temperature in a month i. Here, obs for observed, and mod for model simulated before bias-correction.

2.3. Description of SWAT model

The SWAT model has been used to assess the hydrological responses of complex and large watersheds in different regions of the world. The SWAT literature database for peer-reviewed journal articles can be referenced to at (https://www.card.iastate.edu/swat_articles/). The SWAT model is easily and publicly available and recreates the main hydrological processes in the watersheds. Using the SWAT model increases the level of detail in temporal and geographical variability in ecosystem service. The SWAT model is developed to simulate hydrological parameters in an area where land use land cover is dominated by agricultural land. The Gilgel Gibe-1 watershed is also dominated by agricultural land, so the model can be used. The model applicability can also be calibrated using SWAT CUP [35].

The SWAT model is semi-physically based and enables a high level of spatial detail to be simulated by dividing the watershed into a large number of sub-watersheds, which are further subdivided into Hydrologic Response Units (HRUs) based on soil, LULC, and slope. In this study, the Gilgel Gibe-1 watershed was delineated and then divided into 27 sub-basins (Fig. 1). For HRU definition, the multiple slope option (an option that considers different slope classes for HRU definition) with three slope classes with the slope range of (0–6%, 6–10, and greater than 10 were selected in this watershed. According to Ref. [36], three or less than three slope classes are sufficient for most situations. To avoid small HRUs and to include the required area, a threshold value of 5–10% is usually used in HRU definition [37–40]. In this study 20% threshold value for land use, 15% for soil, and 10% for slope were used. Finally, the Gilgel Gibe-1watershed was subdivided into 187 HRUs.

The major components of SWAT include hydrology, weather, erosion, plant growth, nutrients, pesticides, land management, and stream routing [41,42]. The hydrological processes are simulated for each of HRUs.

The hydrologic continuity equation, also called the water balance equation, used to calculate the hydrological components of the watershed [35] is given in Equation (1):

$$SW_t = SW_0 + \sum_{i=1}^{t} \left(R_{day} - Q_{surf} - Ea - w_{seep} - Q_{gw} \right) \tag{1}$$

In which, SW_t is the final soil water content (mm H$_2$O), SW_0 is the initial soil water content in day i (mm H$_2$O), t is the time (days), R_{day} is the amount of precipitation in day I (mm H$_2$O), Q_{surf} is the $Surf_Q$ in day i (mm H$_2$O), Ea is the ET in day i (mm water), W_{seep} is the percolation in day i (mm H$_2$O), and Q_{gw} is the return flow in a day i (mm H$_2$O).

The SWAT model simulates SurfQ and peak runoff rates for each (HRU) using daily rainfall data and the Soil Conservation Service (SCS) curve number (CN) [35] given in Equation (2). HRU denotes the smallest area, which is made up of LULC, soil type, and slope.

$$Q_{surf} = \frac{\left(R_{day} - I_a \right)^2}{\left(R_{day} - I_a + S \right)} \tag{2}$$

where Q_{surf} is the accumulated runoff or excess rainfall (mm), R_{day} is the rainfall depth for the day (mm), I_a is the initial abstraction that includes surface storage, interception, and infiltration prior to runoff (mm H$_2$O) and S is the retention parameter (mm H$_2$O).

Among the three alternative methods for estimating the potential ET in the SWAT model, namely the Hargreaves, Pristley-Taylor, and Penman-Monteith, the Penman-Monteith method was used in this study.

The Modified Universal Soil Loss Equation (MUSCLE) [43] is used by the SWAT model to calculate surface erosion within each HRU (Equation (3)).

$$sed = 11.8 \left(Q_{surf}.q_{peak}.area_{hru} \right)^{0.56} .K_{USLE}.C_{USLE}.P_{USLE.}.LS_{USLE}.CFRG \tag{3}$$

For details on Equation (3), reference can be made to Ref. [35].

SWAT computes the peak runoff rate with a modified rational method for each HRU as follow [44].

$$Qpeak = \frac{\alpha_{tc} \; * \; Q_{surf} \; * \; A}{t_{con}} \tag{4}$$

where Q_{peak} is peak runoff rate (m^3/s), α_{tc} is the fraction of daily rainfall that occurs during the time of concentration, Q_{surf} is the surface runoff (mm); A is the sub-basin area (km^2), t_{con} is a time of concentration (hr)

2.4. SWAT calibration and performance analysis

The parameter sensitivity analysis, calibration, validation, and uncertainty analysis for the SWAT model were performed using the SWAT-CUP developed by Karim Abbaspour [41]. The model's sensitivity to changes in parameters was evaluated and ranked before calibration and validation.

Among the five optimization methods found in the SWAT-CUP namelyGLUE, Para Sol, SUFI2, MCMC, and PSO, SUFI2 has been widely applied by researchers and SUFI2 was used for this study. The SUFI-2 algorithm accounts for a variety of sources of uncertainty, including uncertainty in driving variables (for example, precipitation (rainfall)), conceptual models, parameters, and observed data. A P-factor, which is the percentage of observed data that is encompassed by the 95% prediction uncertainty, measures the degree to which uncertainties are variably accounted for (95PPU). The 95PPU is calculated using the cumulative distribution of the output generated using the Latin Hypercube sampling at the 2.5% and 97.5% levels [4,41].

To execute the global sensitivity analysis twenty stream flows sensitive parameters were selected. The most sensitive parameters are identified using two indicators, t, and p. p shows the importance of sensitivity while t indicates the degree of sensitivity. The larger the absolute value of t or the smaller the absolute value of p (close to zero), the more sensitive the parameters [45,46]. For example, curve number II (CN2) and GroundWater Delay (GW_DELAY) have a large value for t and a small value for p. This shows that the parameters are more sensitive than the others in the study's watershed.

2.5. Model performance analysis

To evaluate the model's capability for simulating streamflow, The Nash Sutcliff Efficiency (NSE) that goes from - (negative infinity) to 1 (inclusive), and coefficient of determination (R^2) that ranges from 0 to 1 were used. The Model performance improves when the NSE and R^2 are higher and can be judged as satisfactory when NSE >0.50 [47]. Equations (5) and (6) are used to express NSE and R^2.

$$NSE = 1 - \left[\frac{\sum_{i=1}^{n}(Qoi - Qsi)^2}{\sum_{i=1}^{n}(Qoi - \overline{Q}o)^2} \right] \tag{5}$$

Table 1
Percentage change in monthly rainfall under RCP4.5 and RCP8.5

Months	Asendabo		Jimma		Sekoru	
	RCP8.5	RCP4.5	RCP8.5	RCP4.5	RCP8.5	RCP4.5
Jan	−15.28	13.06	−38.11	−28.74	11.54	−0.47
Feb	18.78	−18.95	−22.08	−27.60	37.13	39.98
Mar	−64.63	−77.42	−63.62	−76.66	−70.53	−84.42
Apr	−44.57	−52.15	−59.43	−59.45	−39.26	−49.44
May	−16.29	−21.66	−12.29	−20.77	−20.97	−30.06
Jun	−29.73	−31.68	−25.88	−27.96	−25.41	−26.99
Jul	−8.83	−10.87	−6.75	−2.09	−33.76	−27.85
Aug	5.11	1.97	15.30	9.94	11.37	7.14
Sep	63.69	45.68	39.80	30.45	61.00	47.65
Oct	91.92	87.79	142.18	139.93	202.08	182.73
Nov	200.68	235.23	53.59	75.93	135.88	153.17
Dec	46.33	51.58	19.68	26.23	41.80	40.29

Table 2
Change in temperature (^{o}C) at Asendabo, Jimma and Sekoru stations.

Months	Asendabo				Jimma				Sekoru			
	Tmax		Tmin		Tmax		Tmin		Tmax		Tmin	
	RCP8.5	RCP4.5	RCP8.5	RCP4.5	RCP8.5	RCP4.5	RCP8.5	RCP4.5	RCP8.5	RCP4.5	RCP8.5	RCP4.5
Jan	1.25	1.00	1.04	0.73	1.29	1.11	1.44	1.02	1.24	0.99	1.07	0.93
Feb	1.25	1.06	1.55	0.55	1.25	1.16	1.80	1.11	1.22	1.02	1.48	1.06
Mar	1.27	1.03	1.52	0.73	1.33	1.19	1.79	1.22	1.27	1.06	1.48	1.15
Apr	1.30	1.22	1.23	0.85	1.39	1.39	1.54	0.91	1.27	1.21	1.22	0.92
May	1.62	1.33	1.18	0.93	1.61	1.33	1.46	0.91	1.61	1.32	1.22	0.97
Jun	1.52	1.50	1.23	1.68	1.45	1.55	1.55	1.08	1.53	1.52	1.27	1.14
Jul	1.31	1.15	1.16	1.79	1.26	1.14	1.45	0.94	1.31	1.17	1.21	1.00
Aug	1.23	1.08	1.14	1.84	1.19	1.11	1.44	0.93	1.25	1.10	1.19	0.99
Sep	1.45	0.97	1.09	1.67	1.43	1.01	1.37	0.83	1.45	0.94	1.13	0.86
Oct	1.05	0.83	1.21	1.44	1.05	0.85	1.47	0.97	1.03	0.80	1.22	1.03
Nov	1.13	1.09	0.74	0.70	1.20	1.13	1.11	0.57	1.08	1.05	0.79	0.69
Dec	1.17	1.09	0.10	0.52	1.24	1.18	1.45	0.71	1.15	1.08	1.07	0.80

$$R^2 = \frac{\left[\sum_{i=1}^{n}(Qsi - \overline{Q}s)(Qoi - \overline{Q}o)\right]^2}{\sum_{i=1}^{n}(Qsi - \overline{Q}s)^2 \sum_{i=1}^{n}(Qoi - \overline{Q}o)^2} \tag{6}$$

where; *Qsi*, *Qoi*: the simulated and observed streamflow values, $\overline{Q}o$, $\overline{Q}s$ the mean of the observed and simulated values.
Following model evaluation performance ratings were established for each recommended statistic.

3. Result and discussion

3.1. Climate change analysis

From the analysis of the rainfall in the study area, it is expected that there is an increase in rainfall from August to December, while it decreases from February to July. The maximum decline in rainfall is observed in March and April. For instance, under RCP4.5 a maximum percentage decline of 77.4%, 76.6%, and 84.4% is expected at Asendabo, Jimma, and Sekoru stations respectively. On the other hand, a maximum increase of 235.2%, 139.9%, and 153.2% under RCP4.5 is expected to occur at Asendabo, Jimma, and Sekoru stations in Nov for Asendabo and Sekoru while it is in October for Jimma station. The maximum decrease in rainfall under RCP8.5 is expected in March, with percentage declines of 64.6%, 63.6%, and 70.5% at Asendabo, Jimma, and Sekoru stations, respectively. In the same months as RCP4.5, an increase in rainfall of 200.7%, 142.2%, and 135.9% is expected at Asendabo, Jimma, and Sekoru stations. Generally, rainfall is expected to increase over Gilgel Gibe-1 watershed in the future period of 2026–2055. The predicted increase in monthly rainfall for the future period of 2026–2055 under RCP8.5 is greater than that of RCP4.5. The percentage change in monthly rainfall under RCP4.5 and RCP8.5 with respect to historical is shown in Table 1.

For both RCP4.5 and RCP8.5, the examination of expected maximum and minimum temperatures revealed an increase in temperature. At all stations, the increase in temperature under RCP8.5 is more than that under RCP4.5, except for Asendabo stations, where the increase in minimum temperature under RCP4.5 is greater than that under RCP8.5 for July, August, September, and October. The maximum temperature is predicted to increase within the range of 0.75 °C–1.20 °C for January, February, June, August, September, November, and December at Jimma station under RCP4.5. An increase in maximum temperature in the range of 0.80 °C–1.35 °C for January, February, June, July, August, September, November, and December. At Sekoru station, an increase in
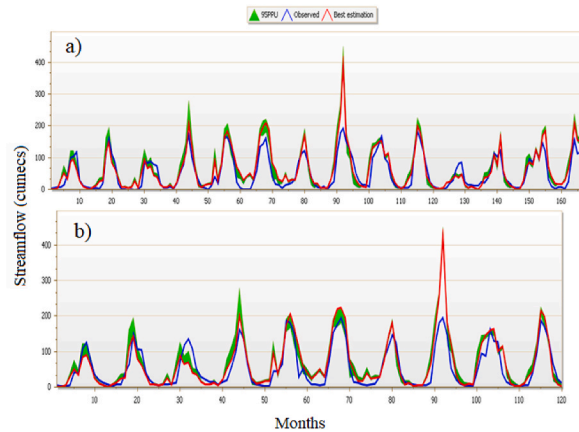
Fig. 3. (a) Stream flow calibration (b) stream flow validation.
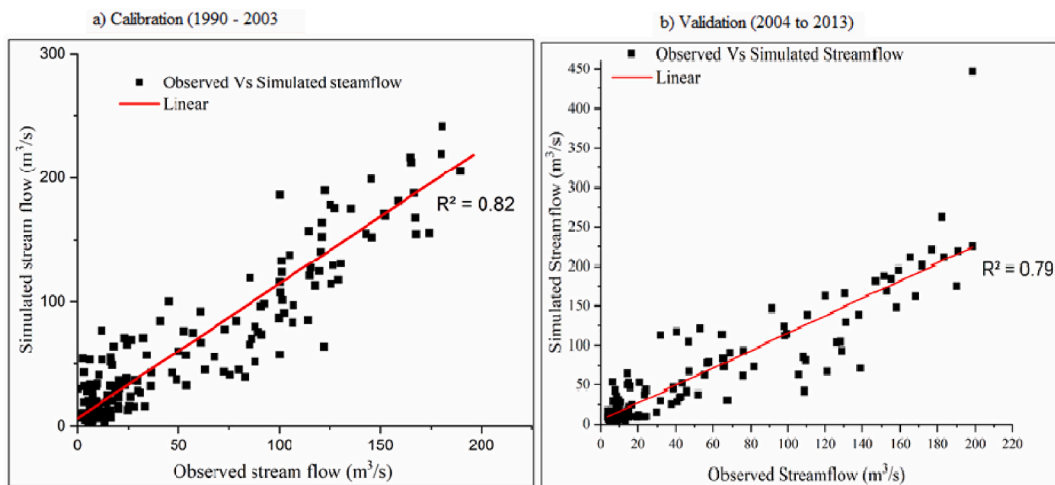
Fig. 4. Scatter plot of observed vs simulated stream flow (a) for calibration and (b) for validation.

maximum temperature predicted under RCP4.5 is 1.52 °C under RCP4.5 and 1.61 under RCP8.5. At Asendabo station, under RCP8.5, the maximum temperature expected to increase with maximum of 1.62 °C in May, however, under RCP4.5 expected to increase will be 1.50 °C in June. Table 2 shows change in temperature (°C) in upper Gilgel Gibe stations.

3.2. Streamflow sensitivity analysis

Using SUFI 2 Global Sensitivity Analysis, nineteen parameters were selected for stream flow sensitivity analysis. The sensitivity ranks for stream flow parameters were based on the p and t values. The bigger the absolute value of t and the smaller p-value the more the sensitivity of the parameter or the smaller absolute value of t and the bigger value of p the less sensitivity of the parameters. CN2 was the most sensitive stream flow parameter in the Gilgel Gibe-1watershed. Table S5 shows the sensitivity rank of the stream flow parameters.

3.2.1. Stream flow calibration and validation

Based on their sensitivity rank, twelve sensitivity parameters for stream flow calibration and validation were chosen (Table S6). The calibration and validation period for stream flow is based on available data. The calibration year is typically greater than the validation year, the majority of studies use 60% of the data for calibration and 40% for validation [48–51]. In this study, 40% of the streamflow was utilized for validation, while 60% was used for calibration.

For model calibration, parameter values were adjusted iteratively within permitted ranges until the measured and simulated streamflow data agreed satisfactorily. The parameters were then fixed, and the model was validated using another set of recorded data. During calibration, the R^2 value was 0.82 and the NSE value was 0.72, while during model validation, the R^2 value was 0.79 and the NSE value was 0.67. These results reveal a strong connection between observed and simulated streamflow, indicating that the SWAT

Table 3

Percentage change in Hydrological components under RCP4.5 and RCP8.5

Months	RCP4.5				
	SURFQ (%)	LAT (%)	Water yield (%)	ET in (%)	Sed yield (%)
Jan	−76.32	19.31	151.38	4.27	−80.00
Feb	95.45	17.53	82.55	−9.09	0.00
Mar	−96.51	−59.53	−44.32	−27.64	−96.43
Apr	−97.91	−62.52	−82.00	−18.33	−98.09
May	−78.69	−41.93	−73.80	−10.01	−80.00
Jun	−70.30	−41.60	−73.34	2.70	−72.12
Jul	−7.74	−20.27	−38.87	0.78	3.76
Aug	15.06	7.10	−14.82	−30.64	12.72
Sep	104.53	25.06	16.39	9.28	104.56
Oct	307.22	54.50	36.66	68.84	371.28
Nov	365.05	105.34	58.76	63.88	436.00
Dec	352.63	41.12	82.82	24.52	266.67
Months	RCP8.5				
	SURFQ (%)	LAT (%)	Water yield (%)	ET in (%)	Sed yield (%)
Jan	57.89	16.55	151.79	−5.66	80
Feb	263.64	21.65	86.92	−4.46	228.57
Mar	−65.12	−48.37	−32.95	−16.84	−53.57
Apr	−96.9	−58.45	−80.43	−16.43	−96.82
May	−68.95	−32.06	−65.58	−8.15	−71.29
Jun	−66.51	−37.04	−67.49	3.23	−69.32
Jul	−21.57	−17.15	−40.11	−5.16	−13.01
Aug	28.87	11.26	−6.15	−32.61	28.5
Sep	150.82	32.7	29.51	15.79	157.19
Oct	324.42	59.98	43.83	72.57	396.81
Nov	324.73	87.08	59.9	59.56	372
Dec	447.37	39.72	82.2	21.31	433.33

model performed well in the Gilgal Gibe-1 watershed and might be employed for evaluating climate change impact. Fig. 3a) shows stream flow calibration and Fig. 3b) shows stream flow validation.

During model calibration and validation, a scattering plot of observed stream flow vs simulated stream also shows a very excellent relationship between simulated and measured stream flow. Fig. 4a) indicates the scatter plot of observed vs simulated stream flow for calibration and Fig. 4b) shows the scatter plot of observed vs simulated for validation.

During calibration, the average stream flow was found to be 55.48 m^3/s, but the simulated flow was 66.48 m^3/s. The measured stream flow during model validation was 57.72 m^3/s while the simulated values were 68.72 m^3/s. This demonstrated that the model overestimated the streamflow during model calibration and validation.

3.3. Change in the hydrological response under climate change

3.3.1. Monthly change in the hydrological response under climate change

The impacts of climate change on the hydrological components of the Gilgel Gibe-1 watershed were assessed based on the changes in temperature and rainfall over future period from 2026 to 2055. Under RCP4.5 and RCP8.5, the calibrated and validated SWAT model was used to simulate hydrological components for the historical (1976–2005) and future periods. The hydrological parameters modeled under future climate change estimates were then compared to historical rainfall and temperature data simulations.

Under both RCP4.5 and RCP8.5, the percentage change in simulated hydrological components indicated that for March, April, May, June, and July, where the percentage change in rainfall is expected to decrease, the corresponding change in all hydrological parameters, including surface runoff, lateral flow, Water yield, ET, and sediment yield, also decreased. The hydrological characteristics corresponding to August, September, October, November, and December, in which rainfall is anticipated to increase, increased under both RCP4.5 and RCP8.5. Comparing the change in hydrological parameters the decrease for RCP4.5 is higher than that of RCP8.5. The percentage increase is higher under RCP8.5 for months where the simulated hydrological parameters increased. The sensitivity of hydrological parameters to changes in rainfall that would occur during wet seasons is revealed by the observed changes. In rainy months, a minor increase in rainfall resulted in increased surface runoff and sediment yield.

To assess the relative influence of climate change (rainfall, maximum and minimum temperature) under both RCP4.5 and RCP8.5 on the hydrological parameters, the Partial Least Square Regression analysis (PLSR) was used. The PSLR model analysis was carried out using XLSTAT software. The correlation coefficient was used to show the relative effect of each independent variable i.e. the percentage change in rainfall and temperature as shown in Table S7a and Table S7b.

In addition, the percentage change in surface runoff and sediment yield were generally negatively correlated with changes in both maximum temperature and minimum temperature. As compared to the change in minimum temperature, the change in maximum temperature had a strong negative correlation with hydrological parameters. This shows that changes in maximum temperature have a greater impact on hydrological parameters in the basin than changes in minimum temperature. This is consistent with the study carried out by Ref. [2] which reported that each temperature increase of 0.7 °C can result in a decrease of 1.4%–2% in annual runoff and 2%–
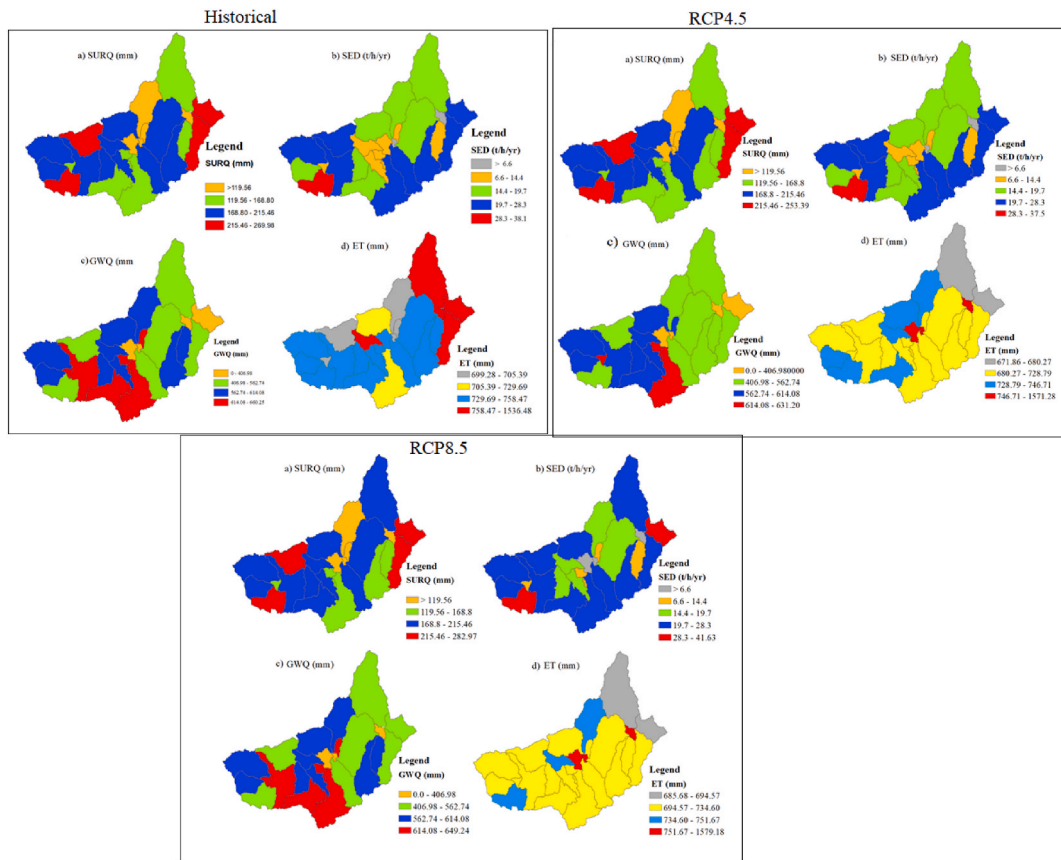
Fig. 5. Hydrological responses at sub basin level under Historical, projected RCP4.5 and RCP8.5: (a) SURQ (mm), (b) SED (t/h/yr), (c) GWQ (mm), (d) ET (mm).

3.7% in annual sediment yield.

The hydrological components under both RCP4.5 and RCP8.5 also revealed a strong positive correlation among themselves except for percentage change in ET and water yield which showed with weak correlation with a coefficient less than 0.5. Table 3 shows the percentage change in hydrological components under RCP4.5 and RCP8.5.

3.3.2. Hydrological components at sub-basin level under climate change

The hydrological components under historical, and projected climate change under both RCP4.5 and RCP 8.5 were evaluated at the sub basin level. The simulated hydrological components such as groundwater, sediment yield, evapotranspiration, and surface runoff using historical, and future scenarios data are shown in Fig. 5. Maximum annual average surface runoff simulated were 269.98 mm, 253.39 mm, and 282.97 mm in sub basin 25 during the historical, RCP4.5, and RCP8.5 respectively. Sediment yield is also high in this sub-basin. This sub-basin is covered by agricultural land and found upstream of the sub-basin. The groundwater flow is high in sub basin 27 (covered by agricultural land use) under the three scenarios. High evapotranspiration is found in sub-basin 4 under the three scenarios.

The sub-basins with high surface runoff and sediment yield under historical climate remained to have the maximum value under projected future climate change. For instance, sub-basins 3,9,15, and 25 had high surface runoff and high sediment yield under historical and RCP4.5 and RCP8.5 projected climate change. When implementing management practices in Gilgel Gibe-1 watershed, priority should be given to these sub-basins. Particularly sub-basins 3 and 9 are close to Gilgel Gibe-1 reservoir and require more attention. Other hydrological parameters such as evapotranspiration will be increased under both scenarios as compared to historical simulations. On contrary, groundwater decreases in values in most sub-basins under climate change. Hydrological responses at sub-basin level under historical, projected RCP4.5 and RCP8.5 are shown in Fig. 5.

3.3.3. Percentage change of hydrological components

As shown in Fig. 6, potential changes in hydrological components under RCP4.5 and RCP8.5 were considered at the sub-basin level. Surface runoff changes from −1.0% to 7.02% under RCP4.5, whereas sediment yield changes from −4.65% to 4.75%. The change in surface runoff is 2.27% more than the change in sediment yield. However, both surface runoff and sediment yield changed within the same range under RCP8.5. −4.76%–9.45%, to be precise. The sediment yield has increased because the expected increase in rainfall
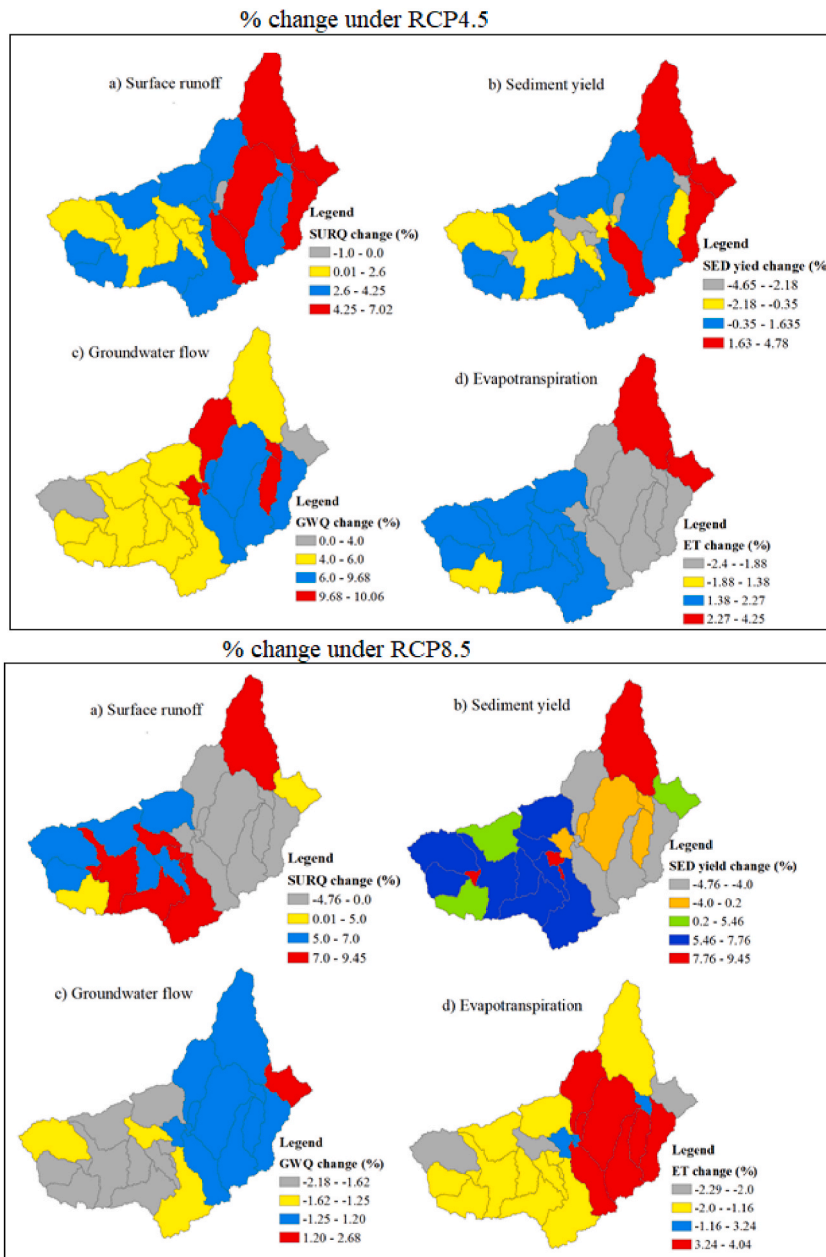
Fig. 6. percent change in hydrologic components under RCP4.5 and RCP8.5 at sub basin level: (a) Surface runoff, (b) sediment yield, (c) Groundwater flow, (d)Evapotranspiration.

under RCP8.5 is greater than that under RCP4.5. Groundwater is projected to vary by a large percentage, while evapotranspiration is expected to change by a minor amount. In comparison to RCP4.5, the changes in hydrological components were significant under RCP8.5. The percentage change in groundwater and Evapotranspiration are low when compared with percentage changes in surface runoff and sediment yield.

The results of this study are consistent with several studies undertaken to evaluate the impact of climate change on hydrological components. For instance, the studies conducted by Refs. [7,52] using RCMs with two Representative Concentration Pathways (RCPs) of 4.5 and 8.5 showed that average monthly streamflow and sediment yield are expected to increase in the future. Similarly, the study conducted by Refs. [23,24] using the CORDEX RCM model to investigate the influence of climate change on hydrological components are found that the mean annual sediment yield and surface runoff is expected to increase in Awash basin, Ethiopia. In addition, the study carried out by Ref. [25] on Finchaa watershed, Ethiopia and [22] on central rift valley basin, Ethiopia, found similar results using the CORDEX Africa RCM.

4. Conclusions and recommendations

In this study, the effects/impacts of climate change on the hydrological components of the Gigel Gibe-1 watershed in Ethiopia were investigated. Under both RCP4.5 and RCP8.5, the corresponding change in all hydrological components dropped during months with expected decreases in rainfall. However, under both RCP4.5 and RCP8.5, modeled hydrological components were raised for months with predicted increases in rainfall.

Additionally, the Partial Least Square Regression analysis was used effectively to assess the relative effect of climate change on hydrological components under both RCP4.5 and RCP8.5.

The percentage change in surface runoff and sediment yield was often inversely proportional to the change in maximum and minimum temperatures. The change in maximum temperature demonstrated a strong negative correlation with hydrological components compared to the change in minimum temperature.

At the spatial scale, the sub-basins with high surface runoff and sediment yield under historical climate remained to have the maximum simulated values under projected future climate change. For instance, sub-basins 3,9,15, and 25 had high surface runoff and high sediment yield under historical, and the same was true under RCP4.5 and RCP8.5 predicted climate change. These sub-basins are completely covered by agricultural land use types. Dystric nitisols and dystric fluvisols are the dominant soil types in these sub basins.

In general, the likely increase in temperature and rainfall in the Gilgel Gibe-1 watershed could increase surface runoff and sediment yield, rendering the watershed sensitive to climate change. The life span of the Gilgel Gibe-1 hydropower reservoir could be shortened due to increased sediment yield. This has to further investigated using the sediment balance of the reservoir. In this study, the impact of Land use/Land cover change was not investigated and future studies should consider both the impacts of climate change and Land use/land cover change on hydrological components.

Author contribution statement

Tamene Adugna Demissie: Conceived and designed the experiments; Performed the experiments; Analyzed and interpreted the data; Contributed reagents, materials, analysis tools or data; Wrote the paper.

Data availability statement

The data that has been used is confidential.

Declaration of competing interest

The authors declare that they have no known competing financial interests or personal relationships that could have appeared to influence the work reported in this paper

Appendix A. Supplementary data

Supplementary data to this article can be found online at https://doi.org/10.1016/j.heliyon.2023.e16701.

References

[1] A. Martínez-Salvador, A. Millares, J.P.C. Eekhout, C. Conesa-García, Assessment of streamflow from EURO-CORDEX regional climate simulations in semi-arid catchments using the SWAT model, Sustainability 13 (2021) 7120, https://doi.org/10.3390/su13137120.

[2] S. Zhang, Z. Li, X. Lin, C. Zhang, Assessment of climate change and associated vegetation cover change on watershed-scale runoff and sediment yield, Water 11 (2019) 1373, https://doi.org/10.3390/w11071373.

[3] X. Zhang, R. Srinivasan, F. Hao, Predicting hydrologic response to climate change in the Luohe River basin using the SWAT model, Trans. ASABE 50 (3) (2007) 901–910.

[4] T.A. Demissie, F. Saathoff, Y. Sileshi, A. Gebissa, Trends of hydro-meteorological data and impact of climate change on the stream flow of Gilgel Gibe 1 River Basin, Ethiopia, Int. J. Curr. Res. 5 (2013) 2988–2993.

[5] IPCC, Climate Change 2014 Synthesis Report Summary for Policy Makers AR5_SYR_FINAL_SPM.pdf (ipcc.Ch), 2014.

[6] IPCC, in: V. Masson-Delmotte, P. Zhai, A. Pirani, S.L. Connors, C. Péan, S. Berger, N. Caud, Y. Chen, L. Goldfarb, M.I. Gomis, M. Huang, K. Leitzell, E. Lonnoy, J. B.R. Matthews, T.K. Maycock, T. Waterfield, O. Yelekçi, R. Yu, B. Zhou (Eds.), Summary for Policymakers, Climate Change 2021: the Physical Science Basis. Contribution of Working Group I to the Sixth Assessment Report of the Intergovernmental Panel on Climate Change, Cambridge University Press, 2021. In Press.

[7] L. Singh, S. Saravanan, Impact of climate change on hydrology components using CORDEX South Asia climate model in Wunna, Bharathpuzha, and Mahanadi, India, Environ. Monit. Assess. 192 (11) (2020), https://doi.org/10.1007/s10661-020-08637-z.

[8] R. Aggarwal, M. Kaushal, S. Kaur, B. Farmaha, Water resource management for sustainable agriculture in Punjab, India, Water Sci. Technol. 60 (11) (2009) 2905–2911.

[9] M. Ouédraogo, P. Houessionon, R.B. Zougmoré, S.T. Partey, Uptake of climate-smart agricultural technologies and practices: actual and potential adoption rates in the climate-smart village site of Mali, Sustainability 11 (2019) 4710, https://doi.org/10.3390/su11174710.

[10] A. Nebiyu, The Sustainable Use of Soil Resources of Gilgel Gibe Dam Catchment. Proceeding of the National Workshop in Integrated Watershed Management on Gibe-Omo Basin, Jimma University and Gilgel Gibe site, 2010, pp. 39–42.

[11] L. Tamene, S.J. Park, R. Dikau, P.L.G. Vlek, Reservoir siltation in the semi-arid highlands of northern Ethiopia: sediment yield–catchment area relationship and a semi-quantitative approach for predicting sediment yield, Earth Surf. Process. Landforms 31 (2006) 1364–1383, https://doi.org/10.1002/esp.1338.

[12] S. Piao, P. Ciais, Y. Huang, Z. Shen, S. Peng, J. Li, L. Zhou, H. Liu, Y. Ma, Y. Ding, P. Friedlingstein, C. Liu, K. Tan, Y. Yu, T. Zhang, J. Fang, The impacts of climate change on water resources and agriculture in China, Nature 467 (2010), https://doi.org/10.1038/nature09364.

[13] B. Bhatta, S. Shrestha, P.K. Shrestha, R. Talchabhadel, Modelling the impact of past and future climate scenarios on streamflow in a highly mountainous watershed: a case study in the West Seti River Basin, Nepal, Sci. Total Environ. 740 (2020), 140156, https://doi.org/10.1016/j.scitotenv.2020.140156.

[14] S. Shrestha, Binod Bhatta, R. Talchabhadel, S.G.P. Virdis, Integrated assessment of the landuse change and climate change impacts on the sediment yield in the Songkhram River Basin, Thailand, Catena 209 (2022), 105859, https://doi.org/10.1016/j.catena.2021.105859.

[15] T.A. Demissie, C.H. Sime, Assessment of the performance of CORDEX regional climate models in simulating rainfall and air temperature over southwest Ethiopia, Heliyon 7 (8) (2021), e07791, https://doi.org/10.1016/j.heliyon.2021.e07791. ISSN 2405-8440.

[16] E. Aldrian, L. Dümenil-Gates, D. Jacob, R. Podzun, D. Gunawan, Long-term simulation of Indonesian rainfall with the MPI regional model, Clim. Dynam. 22 (8) (2004) 795–814, https://doi.org/10.1007/s00382-004-0418-9.

[17] F. Tangang, J.X. Chung, L. Juneng, Supari, E. Salimun, S.T. Ngai, A.F. Jamaluddin, M.S.F. Mohd, F. Cruz, G. Narisma, J. Santisirisomboon, T. Ngo-Duc, P. Van Tan, P. Singhruck, D. Gunawan, E. Aldrian, A. Sopaheluwakan, N. Grigory, A.R.C. Remedio, D.V. Sein, Projected future changes in rainfall in Southeast Asia based on CORDEX–SEA multi-model simulations, Clim. Dynam. 55 (5–6) (2020) 1247–1267, https://doi.org/10.1007/s00382-020-05322-2.

[18] N. Chokkavarapu, V.R. Mandla, Comparative study of GCMs, RCMs, downscaling and hydrological models: a review toward future climate change impact estimation, SN Appl. Sci. 1 (2019) 1698, https://doi.org/10.1007/s42452-019-1764-x.

[19] P. Zhao, H. Lü, H. Yang, W. Wang, G. Fu, Impacts of climate change on hydrological droughts at basin scale: a case study of the Weihe River Basin, China, Quat. Int. (2019), https://doi.org/10.1016/j.quaint.2019.02.022.

[20] Y. Tramblay, D. Ruelland, S. Somot, R. Bouaicha, E. Servat, High-resolution Med-CORDEX regional climate model simulations for hydrological impact studies: a first evaluation of the ALADIN-Climate model in Morocco, Hydrol. Earth Syst. Sci. 17 (10) (2013) 3721–3739, https://doi.org/10.5194/hess-17-3721-2013.

[21] A. Awotwi, T. Annor, G.K. Anornu, J.A. Quaye-Ballard, J. Agyekum, B. Ampadu, I.K. Nti, M.A. Gyampo, E. Boakye, Climate change impact on streamflow in a tropical basin of Ghana, West Africa, J. Hydrol.: Reg. Stud. 34 (2021), 100805, https://doi.org/10.1016/j.ejrh.2021.100805.

[22] T. Gadissa, M. Nyadawa, F. Behulu, B. Mutua, The effect of climate change on Loss of lake volume: case of sedimentation in Central Rift Valley basin, Ethiopia, Hydrology 5 (2018) 67, https://doi.org/10.3390/hydrology5040067.

[23] N. Tessema, A. Kebede, D. Yadeta, Modelling the effects of climate change on streamflow using climate and hydrological models: the case of the Kesem sub-basin of the Awash River basin, Ethiopia, Int. J. River Basin Manag. (2020) 1–12, https://doi.org/10.1080/15715124.2020.1755301.

[24] N.B. Jilo, B. Gebremariam, A.E. Harka, G.W. Woldemariam, F. Behulu, Evaluation of the impacts of climate change on sediment yield from the Logiya Watershed, Lower Awash Basin, Ethiopia, Hydrology 6 (2019) 81, https://doi.org/10.3390/hydrology6030081.

[25] W.T. Dibaba, T.A. Demissie, K. Miegel, Drivers and implications of land use/land cover dynamics in Finchaa catchment, Northwestern Ethiopia, Land 9 (2020) 113, https://doi.org/10.3390/land9040113.

[26] A.F. Lutz, H.w.ter Matt, H. Biemans, A.B. Shrestha, P. Wester, W.W. Immerzeel, Selecting Representative climate models for climate change impact studies: an advanced evelope based selection approach, Int. J. Climatol. 36 (2016) 3988–4005. Published online 18 January 2016 in Wiley Online Library.

[27] E. Mutayoba, J.J. Kashaigili, Evaluation for the performance of the CORDEX regional climate models in simulating rainfall characteristics over Mbarali river catchment in the Rufiji Basin, Tanzania, J. Geosci. Environ. Protect. 5 (2017) 139–151, https://doi.org/10.4236/gep.2017.54011.

[28] W.T. Dibaba, K. Miegel, T.A. Demissie, Evaluation of the CORDEX regional climate models performance in simulating climate conditions of two catchments in Upper Blue Nile Basin, Dynam. Atmos. Oceans 87 (2019), 101104, https://doi.org/10.1016/j.dynatmoce.2019.101104.

[29] S. van Vooren, B. Van Schaeybroeck, J. Nyssen, M. Van Ginderachter, P. Termonia, Evaluation of CORDEX rainfall in northwest Ethiopia: sensitivity to the model representation of the orography, Int. J. Climatol. 39 (2019) 2569–2586, https://doi.org/10.1002/joc.5971.

[30] Y. Xin, Linear Regression Analysis: Theory and Computing, vols. 1–2, World Scientific, 2009. ISBN 9789812834119.

[31] C.H. Sime, T.A. Demissie, Assessment and prediction of the climate change impact on crop yield, in Jimma Zone Upper Gilgel Gibe Districts, Ethiopia, Arabian J. Geosci. 15 (3) (2022), https://doi.org/10.1007/s12517-022-09605-2.

[32] U. Ehret, E. Zehe, V. Wulfmeyer, K. Warrach-Sagi, J. Liebert, HESS Opinions "Should we apply bias correction to global and regional climate model data?", Hydrol. Earth Syst. Sci. 16 (2012) 3391–3404, https://doi.org/10.5194/hess-16-3391-2012.

[33] S.C. van Pelt, P. Kabat, H.W. ter Maat, B.J.J.M. van den Hurk, Weerts, Discharge simulations performed with a hydrological model using bias corrected regional climate model input. https://doi.org/10.5194/hessd-6-4589-2009, 2009.

[34] K.D. Kahsay, S.M. Pingale, S.D. Hatiye, Impact of climate change on groundwater recharge and base flow in the sub-catchment of Tekeze basin, Ethiopia, Groundwater Sustain. Dev. 6 (2018) 121–133, https://doi.org/10.1016/j.gsd.2017.12.002.

[35] S.L. Neitsch, J.G. Arnold, J.R. Kiniry, J.R. Williams, Soil and Water Assessment Tool Theoretical Documentation Version 2009, Texas Water Resources Institute, 2011. https://oaktrust.library.tamu.edu/bitstream/handle/1969.1/128050/TR-406_SoilandWaterAssessmentToolTheoreticalDocumentation.pdf?sequence=1.

[36] J.G. Arnold, J.R. Kiniry, R. Srinivasan, J.R. Williams, E.B. Haney, S.L. Neitsch, SWAT Input/output Documentation Version 2012, vol. 654, Texas Water Resources Institute, 2012, pp. 1–646.

[37] P.J. Starks, D.N. Moriasi, Spatial resolution effect of precipitation data on SWAT calibration and performance: implications for CEAP, Trans. ASABE 52 (4) (2009) 1171–1180.

[38] K.J. Tobin, M.E. Bennett, Using SWAT to model streamflow in two river basins with ground and satellite precipitation data, J. Am. Water Resour. Assoc. 45 (1) (2009) 253–271, https://doi.org/10.1111/j.1752-1688.2008.00276.x.

[39] M.M. Kalcic, I. Chaubey, J. Frankenberger, Defining Soil and Water Assessment Tool (SWAT) hydrologic response units (HRUs) by field boundaries, Int. J. Agric. Biol. Eng. 8 (3) (2015) 69–80.

[40] G. Singh, D. Saraswat, A. Sharpley, A sensitivity analysis of impacts of conservation practices on water quality in L'Anguille River Watershed, Arkansas. Water 10 (4) (2018) 443.

[41] K.C. Abbaspour, SWAT-CUP, SWAT Calibration and Uncertainty Programs. A User Manual, Swiss Federal Institute for Aquatic Science and Technology, Zurich, Switzerland, 2007, p. 84, https://doi.org/10.1002/joc.460. https://www.sciencedirect.com/science/article/pii/S2405844021018946. https://wileyonlinelibrary.com.

[42] J.G. Arnold, R. Srinivasan, R.S. Muttiah, J.R. Williams, Large-area hydrologic modeling and assessment: Part I. Model development, J. Am. Water Resour. Assoc. 34 (1) (1998) 73–89.

[43] J.R. Williams, Sediment-yield prediction with universal equation using runoff energy factor. Present and prospective technology for predicting sediment yield and sources, Environ. Sci. 40 (1975) 244.

[44] Robert Rallison, Miller, Norman, Past, present, and future SCS runoff procedure, in: Rainfall-runoff Relationship/proceedings, International Symposium on Rainfall-Runoff Modeling Held May 18-21, 1981 at Mississippi State University, Mississippi State, Mississippi, USA/edited by VP Singh, 1982.

[45] Y. Chen, J. Niu, Y. Sun, Q. Liu, S. Li, P. Li, L. Sun, Q. Li, Study on streamflow response to land use change over the upper reaches of Zhanghe Reservoir in the Yangtze River basin, Geosci. Lett. 7 (1) (2020), https://doi.org/10.1186/s40562-020-00155-7.

[46] Q. Li, J. Zhang, H.L. Gong, Hydrological simulation and parameter uncertainty analysis using SWAT model based on SUIF-2 algorithm for Guishuihe River Basin, J. China Hydrol. 3 (2015) 43–48.

[47] D.N. Moriasi, J.G. Arnold, M.W. Van Liew, R.L. Bingner, R.D. Harmel, T.L. Veith, Model evaluation guidelines for systematic quantification of accuracy in watershed simulations, Trans. ASABE 50 (3) (2007) 885–900.

[48] S. Khatun, M. Sahana, S.K. Jain, N. Jain, Simulation of surface runoff using semi distributed hydrological model for a part of Satluj Basin: parameterization and global sensitivity analysis using SWAT CUP, Model. Earth Syst. Environ. 4 (3) (2018) 1111–1124, https://doi.org/10.1007/s40808-018-0474-5.

[49] B. Das, S. Jain, S. Singh, P. Thakur, Evaluation of multisite performance of SWAT model in the gomti river basin, India, Appl. Water Sci. 9 (5) (2019), https://doi.org/10.1007/s13201-019-1013-x.

[50] F.G. Tufa, C.H. Sime, Stream flow modeling using SWAT model and the model performance evaluation in Toba sub-watershed, Ethiopia, Model, Earth Syst. Environ. 7 (2020) 2653–2665, https://doi.org/10.1007/s40808-020-01039-7.vol.

[51] S.S. Fanta, C.H. Sime, Performance assessment of SWAT and HEC-HMS model for runoff simulation of Toba watershed, Ethiopia, Sustain. Water Resour. Manag. 8 (1) (2021), https://doi.org/10.1007/s40899-021-00596-8.

[52] A.P. Nilawar, M.L. Waikar, Impacts of climate change on streamflow and sediment concentration under RCP 4.5 and 8.5: a case study in Purna river basin, India, Sci. Total Environ. 650 (2019) 2685–2696, https://doi.org/10.1016/j.scitotenv.2018.09.334.